

Indentation hardness, plasticity and initial creep properties of nanosilver sintered joint

Zhang, Hao; Liu, Yang; Wang, Lingen; Sun, Fenglian; Fan, Xuejun; Zhang, Guo Qi

DOI

[10.1016/j.rinp.2018.12.026](https://doi.org/10.1016/j.rinp.2018.12.026)

Publication date

2019

Document Version

Final published version

Published in

Results in Physics

Citation (APA)

Zhang, H., Liu, Y., Wang, L., Sun, F., Fan, X., & Zhang, G. Q. (2019). Indentation hardness, plasticity and initial creep properties of nanosilver sintered joint. *Results in Physics*, 12, 712-717. <https://doi.org/10.1016/j.rinp.2018.12.026>

Important note

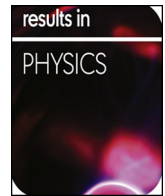
To cite this publication, please use the final published version (if applicable). Please check the document version above.

Copyright

Other than for strictly personal use, it is not permitted to download, forward or distribute the text or part of it, without the consent of the author(s) and/or copyright holder(s), unless the work is under an open content license such as Creative Commons.

Takedown policy

Please contact us and provide details if you believe this document breaches copyrights. We will remove access to the work immediately and investigate your claim.



Indentation hardness, plasticity and initial creep properties of nanosilver sintered joint



Hao Zhang^{a,b,*}, Yang Liu^{a,b}, Lingen Wang^c, Fenglian Sun^b, Xuejun Fan^d, Guoqi Zhang^{a,*}

^a Department of Microelectronics, Delft University of Technology, Delft 2628 CD, the Netherlands

^b School of Materials Science and Engineering, Harbin University of Science and Technology, Harbin 150040, China

^c Boschman Technologies B.V., Duiven 6921 EX, the Netherlands

^d Department of Mechanical Engineering, Lamar University, Beaumont, TX 77710, USA

ARTICLE INFO

Keywords:

Nanosilver
Sintering pressure
Indentation hardness
Plastic deformation
Initial creep

ABSTRACT

The nanoindentation test was conducted in this paper to investigate the indentation hardness, plasticity and initial creep properties of pressure sintered nanosilver joint at various test temperatures. The effects of strain rate on the indentation hardness were first investigated. Then yield stress of nanosilver sintered joint was studied in various pressures sintered joints and the corresponding plastic stress-strain constitutive equations were gained. The maximum indentation depth of nanosilver sintered joint was obviously affected by the test temperature and sintering pressure. The indentation hardness of nanosilver sintered joint decreased with increasing test temperature from 140 to 200°C, which can be attributed to the increased amount of thermal vacancies at high temperatures. However, the indentation modulus exhibited decrease trend as the temperature increased. It is suggested that the distance between adjacent atoms was enlarged at elevated temperatures and furtherly resulted in the decrease of indentation modulus. In addition, the increased sintering pressure from 5 to 30 MPa improved the indentation hardness and modulus of sintered joint. The initial creep was observed in nanosilver sintered joint at temperatures ranged from 140 to 200°C. The increase of sintering pressure improved the resistance to creep of nanosilver sintered joint.

Introduction

Power electronic modules, which are expected to work in severe environments, have been regarded as the critical part in many fields including transportation (hybrid electric vehicles/electric vehicles, traction systems), utilities (smart grids, photovoltaic power and wind power systems), industries (motor drivers, electric machinery) and consumer products (uninterruptible power supplies, battery chargers) [1–3]. The power electronics are generally used to realize the conversion and transmission of electricity [4]. The first level interconnection is usually achieved through a die attach layer between power die and ceramic substrate. Consequently, the die attach layer plays an important role in ensuring the thermal and electrical conduction in power electronic modules. During the operation process of power electronics, temperature change occurs due to the periodical application of electric power [5]. Since the coefficient of thermal expansion is variable in each layer, so thermo-mechanical stress is expected to generate in the die attach layer. Therefore, the thermal reliability of die attach layer greatly affects the performance of power electronics.

The nanosilver sintering technology has gained high popularity in attaching power dies in power electronics packaging [6–8], and the reliability investigation of nanosilver sintered joint has become the mainstream in recent years. Zhao et al. [9] found that the fracture morphology of nanosilver sintered joint exhibited significant plastic flow during shear test, which implied the high bonding strength. Similar result was also obtained by Fu et al. [10]. Bai et al. [11] proved that the dislocation creeps were produced in sintered silver die attach layer during thermal cycling test. The pile-up of dislocation creeps promoted the formation of microcavities at the grain boundaries and finally resulted in the decrease of shear strength. Li et al. [12] investigated the creep behavior of nanosilver sintered lap shear joint, and the results showed that the creep strain of nanosilver sintered joint increased with the increase of temperature from 225 to 325°C. Chen et al. [13] found that the accumulation of creep strain of nanosilver sintered thin film became faster as the temperature increasing from 100 to 175°C. This result indicated that the higher temperature would lead to a shorter creep rupture life. The nanoindentation test method is usually used to characterize the plastic deformation and creep behavior

* Corresponding authors at: Department of Microelectronics, Delft University of Technology, Delft 2628 CD, the Netherlands (H. Zhang).

E-mail addresses: hoayzhang@163.com (H. Zhang), g.q.zhang@tudelft.nl (G. Zhang).

of materials on nano/microscale [14–16]. This technology has been used to investigate the room temperature viscoplastic properties of silver sintered joint [17,18]. However, the silver sintered joint is expected to serve at high temperatures and there are few researches reporting on the high temperature indentation properties of nanosilver sintered joint while incorporating pressure effects.

This paper investigated the indentation hardness, plasticity and initial creep properties of pressure sintered nanosilver joint. The nanosilver sintered joint was evaluated by nanoindentation test at various temperatures. The effects of strain rate on the indentation hardness were first analyzed. Then the elastoplastic behaviors of nanosilver sintered joint at room temperature were discussed. What's more, the temperature dependence of indentation depth, hardness and elastic modulus were studied, respectively. Besides, the effects of temperature on the evolution of initial creep behavior of nanosilver sintered joint were analyzed.

Experimental procedures

The commercial Argomax 2020 (from Alpha Assembly Solutions) [19] nanosilver film with thickness of 65 μm was used as the sintering material. The molybdenum (Mo) coated with (Mo)/Ni/Cu/Ag on both sides was used as substrate. The upper one was named as top Mo substrate and lower one was to be the bottom Mo substrate. The dimension of Mo substrate was 13.60 × 13.60 × 2.00 mm³. The nanosilver film was first transferred to the bottom Mo substrate through lamination process at 130°C and 5 MPa pressure for 2 min. Then the top Mo substrate was placed on the laminated bottom Mo substrate and sintered at 250°C for 3 min with various pressures. The schematic diagram of sintering process was shown in Fig. 1. In order to investigate the effects of pressure on the mechanical properties of nanosilver sintered joint, the sintering pressure was respectively set as 5, 10, 20, 30 MPa for each sintering process. After sintering, the sample was grinded and polished with 0.25 μm suspension of diamond for the nanoindentation test. The scanning electron microscope was also used to examine the morphology of polished sample to ensure the quality of sintered layer. In order to ensure the high accuracy of tests, only the central part of the sintered layer was used in the nanoindentation test.

The SHIMADZU Dynamic Ultra-micro Hardness Tester (DUH-211S) was used to characterize the micro mechanical properties of nanosilver sintered joint. This tester was equipped with the 115° Berkovich indenter. The loading-holding-unloading mode was applied to the test and the holding time was set as 10 s. The indentation test was first conducted at room temperature at 5 mN loading force. The strain rate of 0.004, 0.02, 0.1 and 0.2 s⁻¹ were selected for investigating its effect on indentation hardness. The strain rate is obtained through dividing the loading speed by loading force. The cross section morphology of 30 MPa sintered nanosilver joint was shown in Fig. 2(a). The indentation morphology tested at 25°C and 0.2 s⁻¹ was shown in Fig. 2(b). The high temperature tests were achieved with the help of micro heater assembled in the DUH-211S. The temperature referred here was the temperature on the test sample, which was measured and controlled precisely through the whole indentation test. The test was conducted at 140, 160, 180 and 200°C, respectively. The test force and strain rate for

high temperature test was respectively set as 5 mN and 0.2 s⁻¹. Each data was the average value of at least 9 tests at the same condition. The Oliver and Pharr method was used to determine the hardness and elastic modulus of tested sample [20]. Previous results revealed that the porosity of sintered nanosilver joint decreased from 1.39% to 1.14% as the sintering pressure increased from 5 to 30 MPa [6]. The low porosity as well as the difference of porosity have limited effect on the change of the Poisson's ratio according to the calculation method adopted by Long et al. [21]. So, the Poisson's ratio of 0.37 for pure Ag is used for the nanoindentation tests in this paper.

Results

Effects of strain rate on the evolution of indentation hardness

Since the strain rate plays an important role in determining the mechanical properties of materials [21], the nanosilver sintered joint is tested at 25°C under various strain rates and the results are shown in Fig. 3. With the increase of strain rate from 0.004 to 0.02 s⁻¹, the indentation hardness (H_{IT}) of nanosilver sintered joint increases sharply. However, the increase rate of H_{IT} decreases as the strain rate increasing from 0.02 to 0.1 s⁻¹. Limited effect is observed on H_{IT} when the strain rate reaches 0.2 s⁻¹. It is suggested that the indentation size is larger at low strain rate when comparing with the one tested at high strain rate [22]. According to Eq. (1) [23], the larger indentation size A_c will result in higher indentation hardness H_{IT} at the same loading force F_{max} . This effect becomes insignificant when the strain rate increases to certain level. So the strain rate of 0.2 s⁻¹ is chosen for the following tests.

$$H_{IT} = \frac{F_{max}}{A_c} \tag{1}$$

Plastic stress-strain constitutive model of nanosilver sintered joint at room temperature

During nanoindentation test, the nanosilver sintered joint deforms as the indentation load increases and elastic deformation occurs at the beginning stage. Once the indentation load exceeds the yield strength of sintered joint, plastic deformation happens and leads to the irreversible deformation. Since the residual indentation depth is recorded after the nanoindentation test, so the deformation of nanosilver sintered joint consists of both elastic and plastic deformation. The stress (σ)-strain (ϵ) behavior of sintered joint can be expressed in general form as follows [24–26]:

$$\sigma = \begin{cases} E\epsilon & (\sigma \leq \sigma_y) \\ \sigma_y(1 + \frac{E}{\sigma_y}\epsilon_p)^n & (\sigma > \sigma_y) \end{cases} \tag{2}$$

where E represents the elastic modulus of tested material, σ_y represents the initial yield stress, ϵ_p represents the plastic strain, n represents the strain hardening exponent.

There is an empirical equation describing the relationship between yield stress σ_y and hardness H_{IT} , as seen in Eq. (3) [27]:

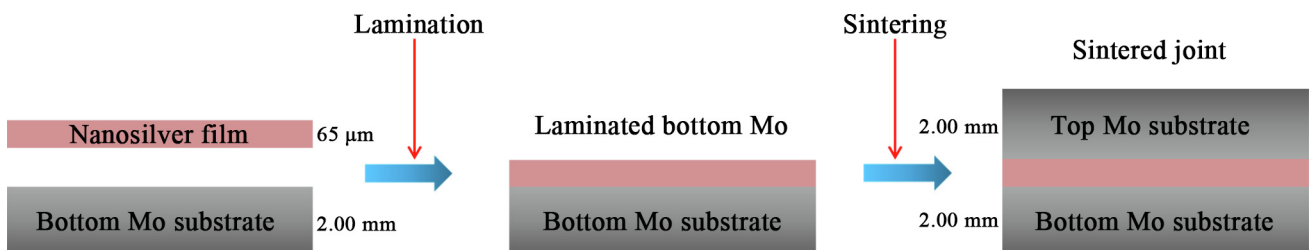


Fig. 1. Schematic diagram of sample structure (not drawn to scale).

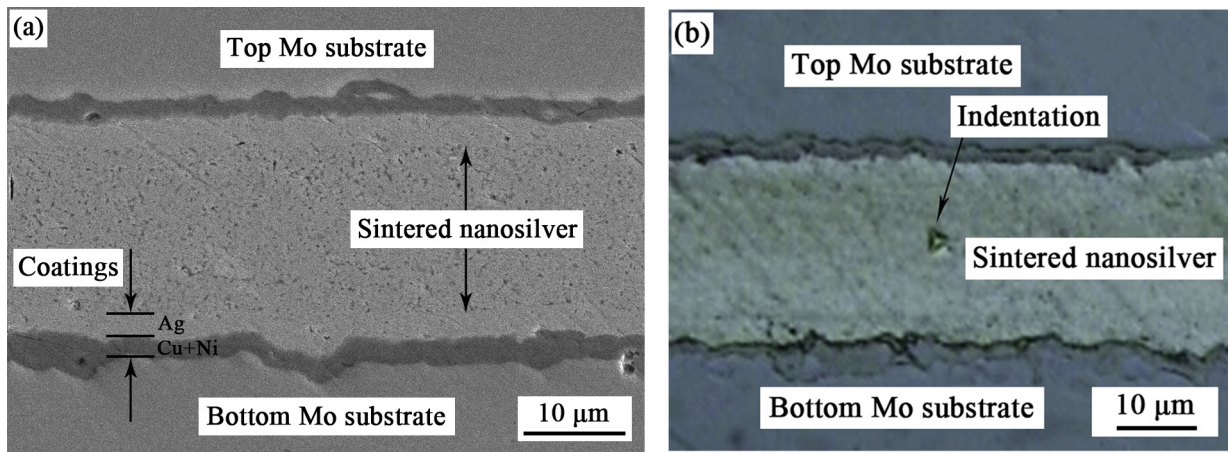


Fig. 2. Morphology of 30 MPa sintered nanosilver joint, (a) cross section, (b) after indentation.

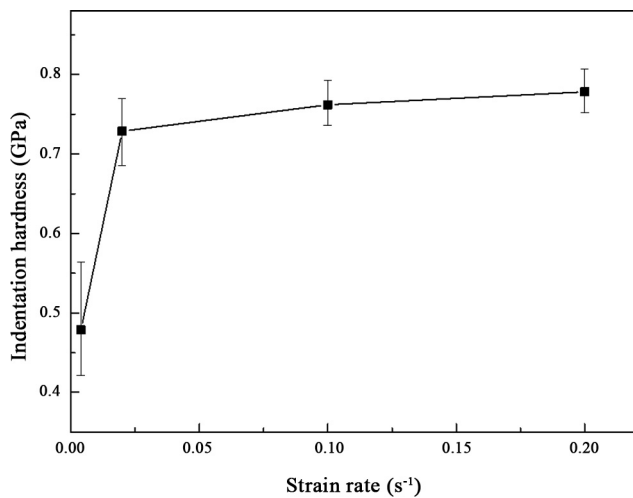


Fig. 3. Relationship between indentation hardness and strain rate of 5 MPa sintered nanosilver joint.

$$\sigma_y \approx \frac{H_{IT}}{3} \quad (3)$$

The strain hardening exponent (n) can be calculated according to literature [28]. The σ_y and n for various pressures sintered nanosilver joint are summarized in Table 1. As the sintering pressure increases from 5 to 30 MPa, the yield stress σ_y of nanosilver sintered joint increases. This result implies that the strength of nanosilver sintered joint can be enhanced by increasing the sintering pressure. In addition, the strain hardening exponent n exhibits increase trend with increasing pressure. The increase of n indicates the increased capability of bearing loading force, which also means the improvement of resistance to plastic deformation. Combining with Eq. (2), the plastic stress-strain constitutive equations of nanosilver sintered joint with various sintering pressures at room temperature are gained and shown in Table 2.

Temperature dependence of indentation depth

Fig. 4 is the evolution of indentation load-depth curve of 5 MPa

Table 1
The σ_y and n of nanosilver sintered joint with various sintering pressures (25°C).

| | 5 MPa | 10 MPa | 20 MPa | 30 MPa |
|------------------|-------|--------|--------|--------|
| σ_y (GPa) | 0.26 | 0.33 | 0.64 | 0.67 |
| n | 0.43 | 0.47 | 0.48 | 0.48 |

Table 2
Plastic stress-strain constitutive equation of nanosilver sintered joint (25°C).

| Sintering pressure | Plastic stress-strain constitutive equation |
|--------------------|--|
| 5 MPa | $\sigma = \begin{cases} 31.72\epsilon & (\sigma \leq 0.26 \text{ GPa}) \\ 0.26(1 + 120.22\epsilon_p)^{0.43} & (\sigma > 0.26 \text{ GPa}) \end{cases}$ |
| 10 MPa | $\sigma = \begin{cases} 39.93\epsilon & (\sigma \leq 0.33 \text{ GPa}) \\ 0.33(1 + 122.65\epsilon_p)^{0.47} & (\sigma > 0.33 \text{ GPa}) \end{cases}$ |
| 20 MPa | $\sigma = \begin{cases} 66.73\epsilon & (\sigma \leq 0.64 \text{ GPa}) \\ 0.64(1 + 104.64\epsilon_p)^{0.48} & (\sigma > 0.64 \text{ GPa}) \end{cases}$ |
| 30 MPa | $\sigma = \begin{cases} 81.83\epsilon & (\sigma \leq 0.67 \text{ GPa}) \\ 0.67(1 + 122.69\epsilon_p)^{0.48} & (\sigma > 0.67 \text{ GPa}) \end{cases}$ |

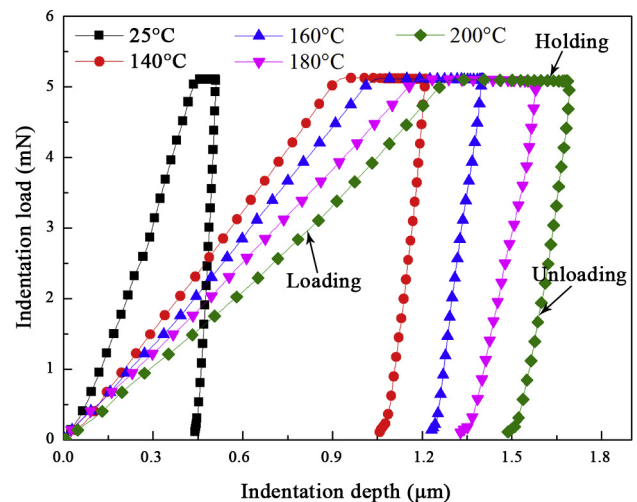


Fig. 4. Indentation load-depth curves of 5 MPa sintered nanosilver joint at various temperatures.

sintered nanosilver joint at 25, 140, 160 and 200°C test temperatures. The indentation load-depth curve consists of three stage, the loading stage, holding stage and unloading stage. As seen in Fig. 4, the maximum indentation depth (h_{max}) increases from 0.51 to 1.81 μm as the test temperature increases from 25 to 200°C. The h_{max} at 200°C is approximately three times higher than that tested at 25°C. Besides, the slope of loading stage becomes smaller at 200°C when comparing to the sample tested at 25°C. Similar trends are also found in 10, 20 and 30 MPa sintered nanosilver joint, but the h_{max} exhibits difference in various pressures sintered nanosilver joint. The corresponding results are summarized in Fig. 5. The difference of h_{max} between 25 and 200°C

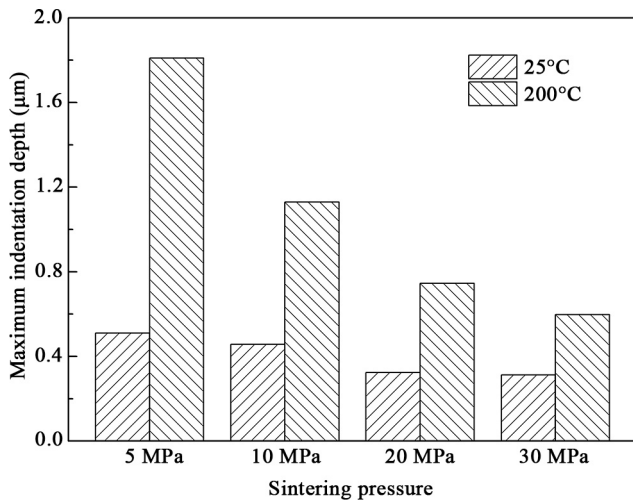


Fig. 5. Effects of temperature and sintering pressure on the maximum indentation depth of nanosilver sintered joints.

in 5, 10, 20 and 30 MPa sintered joint is 1.30, 0.67, 0.43 and 0.29 μm, respectively. The value of difference decreases gradually with the increase of sintering pressure. This result implies that the sensitivity of h_{max} to temperature during nanoindentation test decreases with increasing sintering pressure from 5 to 30 MPa. Meanwhile, the result also indicates that the resistance to elastoplastic deformation of nanosilver sintered joint can be greatly enhanced by increasing the sintering pressure. In the serving process of nanosilver sintered package, stress induced deformation occurs due to the mismatch of coefficients of thermal expansion (CTE). The reliability of nanosilver sintered joint can be improved due to its increased resistance to the deformation when sintered with pressures.

Temperature dependence of indentation hardness

Fig. 6 shows the relationship between indentation hardness (H_{IT}) and test temperature for various pressures sintered joints. With the increase of temperature, the H_{IT} presents decrease trend in all the four pressures sintered joints. This result indicates that the softening phenomenon happens in nanosilver sintered joint at high temperatures. Thus, the resistance to plastic deformation of sintered joint decreases and furtherly leads to the decrease of H_{IT} accordingly. It is suggested that the amount of thermal vacancies is increasing exponentially with

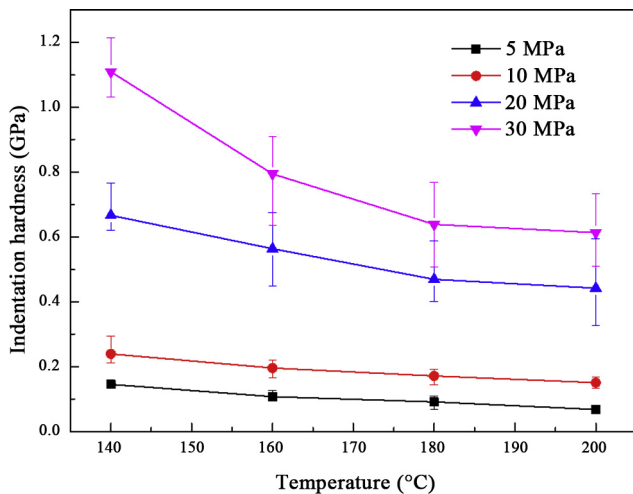


Fig. 6. Relationship between indentation hardness and temperature of pressure sintered nanosilver joint.

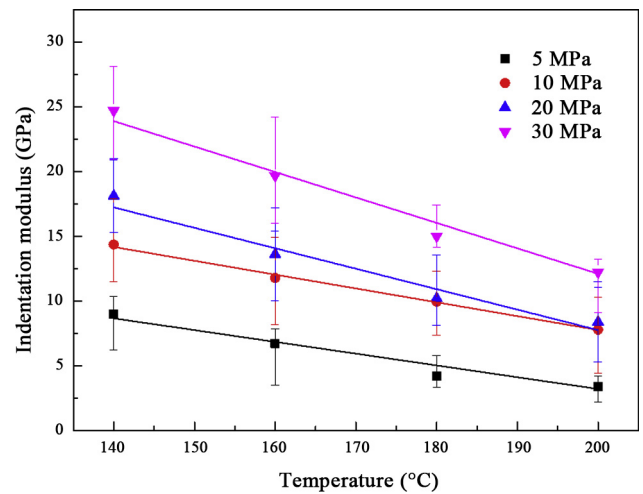


Fig. 7. Relationship between indentation modulus and temperature of sintered nanosilver joint.

temperature [29]. The activity of dislocation can be enhanced by the generated thermal vacancies at elevated temperature and therefore results in the decrease of indentation hardness [30]. In addition, the H_{IT} increases with the increase of sintering pressure at the same test temperature. The diffusion bonding among nanosilver particles can be greatly enhanced with the help of sintering pressure. This will further result in greater number and larger area of sintering necks. The hardness of sintered layer can be improved by the increased bonding quality at high pressures.

Temperature dependence of indentation modulus

The evolution of indentation modulus (E_{IT}) of pressure sintered nanosilver joint at high temperatures is shown in Fig. 7. The E_{IT} increases with the increase of sintering pressure. The E_{IT} of 5 and 30 MPa sintered joint at 140°C is 8.98 and 24.71 GPa, respectively. The E_{IT} has increased 2.75 times when the sintering pressure increases from 5 to 30 MPa. The increase of E_{IT} can be attributed to enhanced bonding between nanosilver particles under high sintering pressures. However, the E_{IT} of pressure sintered nanosilver sintered joint decreases with the increase of temperature from 140 to 200°C, as seen in Fig. 7. Similar trend is observed in all four different pressures sintered joints. It has been revealed that the E_{IT} decreases with increasing temperature T , which can be described as follows [31,32]:

$$E_{IT} = A + B * T \tag{4}$$

where A and B are the constants in the equation, which can be obtained from the fitted curve in Fig. 7. The relationship between E_{IT} and T for various pressures sintered joint is summarized in Table 3. It has been revealed that the elastic modulus of a material is inversely proportional to the distance between adjacent atoms [33]. The distance between atoms in sintered joint becomes larger at elevated temperatures, which will result in the smaller indentation modulus.

Table 3 Relationship between H_{IT} and T for various pressures sintered nanosilver joint.

| Sintering pressure | Relationship between H_{IT} and T |
|--------------------|---|
| 5 MPa | $E_{IT} = 21.41 - 0.09T \quad T \in (140 \sim 200^\circ\text{C})$ |
| 10 MPa | $E_{IT} = 29.14 - 0.11T \quad T \in (140 \sim 200^\circ\text{C})$ |
| 20 MPa | $E_{IT} = 39.36 - 0.16T \quad T \in (140 \sim 200^\circ\text{C})$ |
| 30 MPa | $E_{IT} = 51.43 - 0.20T \quad T \in (140 \sim 200^\circ\text{C})$ |

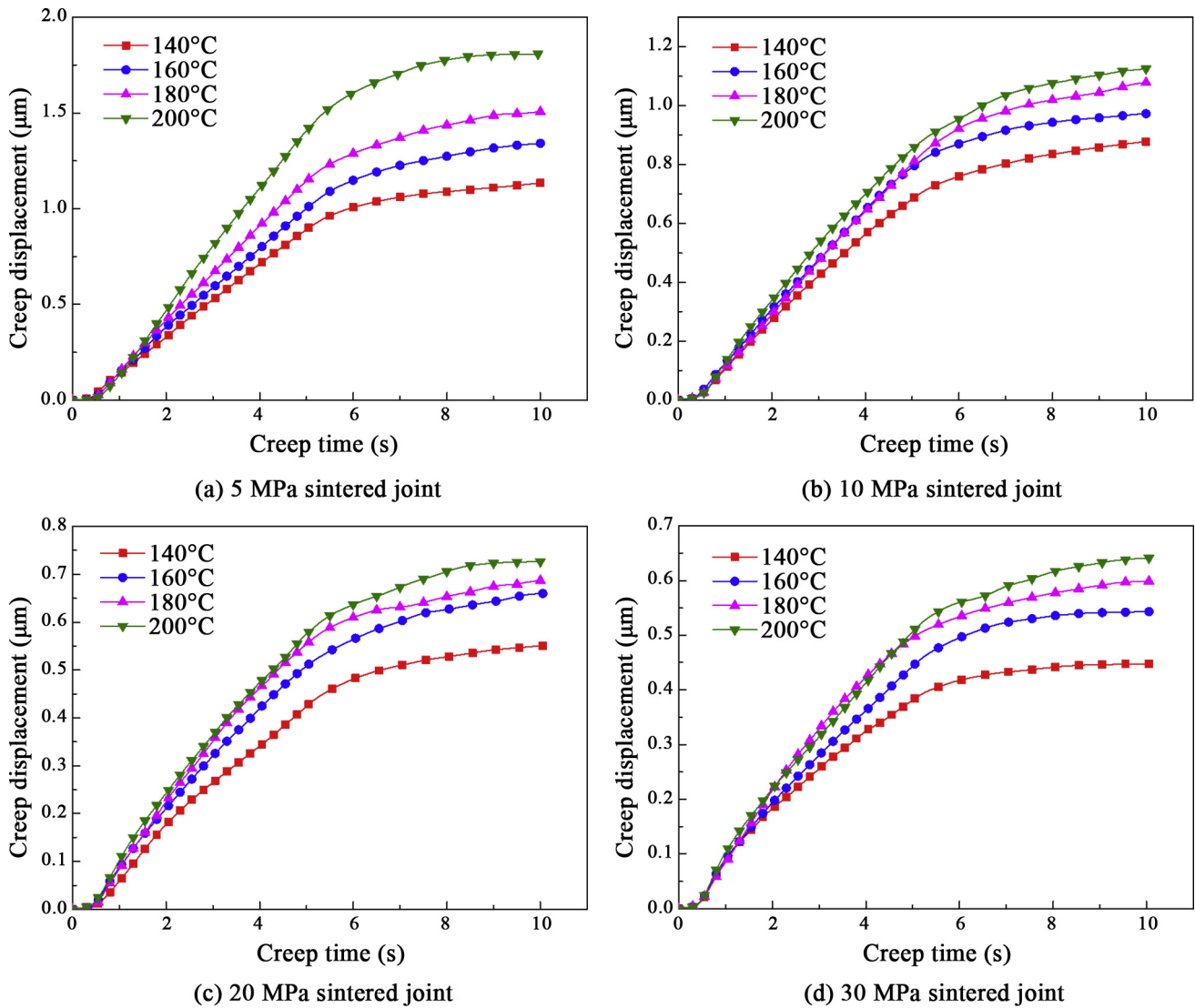


Fig. 8. The creep time-displacement curves of pressure sintered nanosilver joint.

Initial creep behavior of nanosilver sintered joint

The initial creep behavior of nanosilver sintered joint at various temperatures is investigated through nanoindentation test. The creep displacement of nanosilver sintered joint during holding stage is extracted from the load-depth curve and then plotted with creep time. The creep behavior of 5 MPa sintered joint is displayed in Fig. 8(a), the result shows that the evolution of creep displacement exhibits similar trend at four test temperatures. The creep displacement becomes larger as the temperature increasing from 140 to 200°C. The creep displacement increases quickly at the initial creep stage, especially at the first 5 s. The higher the test temperature, the larger the increase rate of initial creep displacement. However, the increase rate of creep displacement decreases gradually after 5 s. As for 10, 20 and 30 MPa nanosilver sintered joint, similar creep law is also observed, as seen in Fig. 8(b), (c) and (d). But the maximum creep displacement after 10 s is quite different in various pressures sintered joint. With the increase of sintering pressure, the maximum creep displacement decreases at the same temperature. The creep displacement at 200°C is much larger than the value obtained at 140°C in 5 MPa sintered nanosilver joint. But this difference becomes quite small in 30 MPa sintered joint, as seen in Fig. 8(a) and (d). These results indicate that the resistance to creep of nanosilver sintered joint can be improved by increasing the sintering

pressure.

Conclusions

The indentation hardness was not greatly affected by the strain rate when it reached 0.2 s^{-1} . Both the yield stress and strain hardening exponent of nanosilver sintered joint increased as the sintering pressure increased from 5 to 30 MPa. The plastic stress-strain constitutive equations of pressure sintered nanosilver joint were obtained at room temperature. The maximum indentation depth of nanosilver sintered joint increased with increasing test temperature from 25 to 200°C, but decreased with increasing sintering pressure from 5 to 30 MPa. Both of the indentation hardness and indentation modulus of nanosilver sintered joint showed decrease trend with the increase of temperature from 140 to 200°C, but increase trend was found when the sintering pressure increased from 5 to 30 MPa. The creep displacement of nanosilver sintered joint increased rapidly at the initial creep stage. The creep displacement of nanosilver sintered joint decreased with the increase of sintering pressure but increased with the increase of temperature.

Acknowledgements

This work is partially supported by the National Natural Science Foundation of China (No. 51174069) and partially supported by the Natural Science Foundation of Heilongjiang Province (No. E2017050).

References

- [1] Zhang G, Li Z, Zhang B, Halang WA. Power electronics converters: Past, present and future; 2017. doi: 10.1016/j.rser.2017.05.290.
- [2] Yoon JW, Lee BS. Sequential interfacial reactions of Au/In/Au transient liquid phase-bonded joints for power electronics applications; 2018. doi: 10.1016/j.tsf.2018.04.039.
- [3] Ji B, Song X, Cao W, Pickert V, Hu Y, Mackersie JW, et al. In situ diagnostics and prognostics of solder fatigue in IGBT modules for electric vehicle drives; 2015. doi: 10.1109/TPEL.2014.2318991.
- [4] Okumura H. A roadmap for future wide bandgap semiconductor power electronics; 2015; doi: 10.1557/mrs.2015.97.
- [5] Lee BS, Yoon JW. Cu-Sn intermetallic compound joints for high-temperature power electronics applications; 2018. doi: 10.1007/s11664-017-5792-2.
- [6] Liu Y, Zhang H, Wang L, Fan X, Zhang G, Sun F. Effect of sintering pressure on the porosity and the shear strength of the pressure-assisted silver sintering bonding; 2018. doi: 10.1109/TDMR.2018.2819431.
- [7] Yu F, Cui J, Zhou Z, Fang K, Johnson RW, Hamilton MC. Reliability of ag sintering for power semiconductor die attach in high-temperature applications; 2017. doi: 10.1109/TPEL.2016.2631128.
- [8] Nishimoto S, Moeini SA, Ohashi T, Nagatomo Y, McCluskey P. Novel silver die-attach technology on silver pre-sintered DBA substrates for high temperature applications; 2018. doi: 10.1016/j.microrel.2018.06.010.
- [9] Zhao SY, Li X, Mei YH, Lu GQ. Study on high temperature bonding reliability of sintered nano-silver joint on bare copper plate; 2015. doi: 10.1016/j.microrel.2015.10.017.
- [10] Fu S, Mei Y, Lu GQ, Li X, Chen G, Chen X. Pressureless sintering of nanosilver paste at low temperature to join large area ($\geq 100 \text{ mm}^2$) power chips for electronic packaging; 2014. doi: 10.1016/j.matlet.2014.04.127.
- [11] Bai JG, Lu GQ. Thermomechanical reliability of low-temperature sintered silver die attached SiC power device assembly; 2006. doi: 10.1109/TDMR.2006.882196.
- [12] Li X, Chen G, Wang L, Mei YH, Chen X, Lu GQ. Creep properties of low-temperature sintered nano-silver lap shear joints; 2013. doi: 10.1016/j.msea.2013.05.001.
- [13] Chen G, Sun XH, Nie P, Mei YH, Lu GQ, Chen X. High-temperature creep behavior of low-temperature-sintered nano-silver paste films; 2012. doi: 10.1007/s11664-012-1903-2.
- [14] Kang NR, Gwak EJ, Jeon H, Song E, Kim JY. Microstructural effect on time-dependent plasticity of nanoporous gold; 2018. doi: 10.1016/j.ijplas.2018.05.011.
- [15] Kong X, Sun F, Yang M, Liu Y. High temperature creep properties of low-Ag Cu/Sn-Ag-Cu-Bi-Ni/Cu solder joints by nanoindentation method; 2016. doi: 10.1108/SSMT-01-2016-0001.
- [16] Elbarbary M. Elasto-plastic material properties of lead-free solder by finite element analysis and nanoindentation test. Master thesis, Lamar University, Beaumont; 2018.
- [17] Leslie D, Dasgupta A, Morillo C. Viscoplastic properties of pressure-less sintered silver materials using indentation; 2017. doi: 10.1016/j.microrel.2017.04.009.
- [18] Kraft S, Zischler S, Tham N, Schletz A. Properties of a novel silver sintering die attach material for high temperature-high lifetime applications; 2013. doi: 10.5162/sensor2013/B3.3.
- [19] Henaff FL, Azzopardi S, Woïgard E, Youssef T, Bontemps S, Joguet J. Lifetime evaluation of nanoscale silver sintered power modules for automotive application based on experiments and finite-element modeling; 2015. doi: 10.1109/TDMR.2015.2443055.
- [20] Oliver WC, Pharr GM. An improved technique for determining hardness and elastic modulus using load and displacement sensing indentation experiments; 1992. doi: 10.1557/JMR.1992.1564.
- [21] Long X, Tang W, Feng Y, Chang C, Keer LM, Yao Y. Strain rate sensitivity of sintered silver nanoparticles using rate-jump indentation; 2018. doi: 10.1016/j.ijmecs.2018.02.035.
- [22] Xiao G, Yuan G, Jia C, Yang X, Li Z, Shu X. Strain rate sensitivity of Sn–3.0 Ag–0.5 Cu solder investigated by nanoindentation; 2014. doi: 10.1016/j.msea.2014.06.113.
- [23] Hou XD, Jennett NM. A method to separate and quantify the effects of indentation size, residual stress and plastic damage when mapping properties using instrumented indentation; 2017. doi: 10.1088/1361-6463/aa8a22.
- [24] Luo J, Lin J. A study on the determination of plastic properties of metals by instrumented indentation using two sharp indenters; 2007. doi: 10.1016/j.ijsolstr.2007.01.029.
- [25] Dao M, Chollacoop N, Vliet KJ, Venkatesh TA, Suresh S. Computational modeling of the forward and reverse problems in instrumented sharp indentation; 2001. doi: 10.1016/S1359-6454(01)00295-6.
- [26] Barbary ME, Chen L, Liu Y, Qin F, Fan X. On the uniqueness and sensitivity of nanoindentation testing for determining elastic and plastic material properties of electroplating copper filled in through-silicon-via (TSV); 2018. doi: 10.1109/ECTC.2018.00157.
- [27] Sanders PG, Youngdahl CJ, Weertman JR. The strength of nanocrystalline metals with and without flaws; 1997. doi: 10.1016/S0921-5093(97)00185-8.
- [28] Giannakopoulos AE, Suresh S. Determination of elastoplastic properties by instrumented sharp indentation; 1999. doi: 10.1016/S1359-6462(99)00011-1.
- [29] George EP, Baker I. Thermal vacancies and the yield anomaly of FeAl; 1998. doi: 10.1016/S0966-9795(98)00063-6.
- [30] Mu D, Huang H, McDonald SD, Nogita K. Creep and mechanical properties of Cu₆Sn₅ and (Cu, Ni)₆Sn₅ at elevated temperatures; 2013. doi: 10.1007/s11664-012-2227-y.
- [31] Kese K, Olsson PAT, Holston AMA, Broitman E. High temperature nanoindentation hardness and Young's modulus measurement in a neutron-irradiated fuel cladding material; 2017. doi: 10.1016/j.jnucmat.2017.02.014.
- [32] Mohamed RM, Mishra MK, Harbi LMA, Ghamdi MSA, Asiri AM, Reddy CM, et al. Temperature dependence of mechanical properties in molecular crystals; 2015. doi: 10.1021/acs.cgd.5b00245.
- [33] Ma H, Suhling JC. A review of mechanical properties of lead-free solders for electronic packaging; 2009. doi: 10.1007/s10853-008-3125-9.